J. Chem. Soc., Faraday Trans. 1, 1988, **84**(7), 2397–2407

Ammoxidation of 2-Methylpyrazine

Characterisation of Catalyst

Lucio Forni,* Cesare Oliva and Claudio Rebuscini

Dipartimento di Chimica Fisica ed Elettrochimica, Università di Milano, Via C. Golgi, 19 I-20133 Milano, Italy

The effect of changing the relative ratios of the active components in Sb–V–Mn mixed oxides, their concentration on the support and the nature of the latter has been analysed by employing several techniques, such as X-ray diffraction, scanning electron microscopy, electron probe microanalysis and electron spin resonance spectroscopy, together with chemical analysis, a titration of the surface acidity, and determinations of both the B.E.T. surface area and the porosity. A close dependence of activity and selectivity on the nature of the support was observed, connected with the ability of the latter to suppress the formation of microporosity. The catalytic activity is due to Sb^{4+} species. V and Mn both act as a structural promoter, conferring electrical conductivity on the solid and so improving the rapid electron transfer from the bulk to the surface, and *vice versa*.

Explorative research carried out in this laboratory has shown that a mixture of Sb, V and Mn oxides is an effective and selective catalyst for the vapour-phase ammoxidation of 2-methylpyrazine (MP) to 2-cyanopyrazine (CP). In this study as many as 35 different catalysts were tested, and the screening was carried out essentially on the base of their behaviour under similar conditions.[1] In the present paper a more systematic approach is followed, by analysing the effect of changing the ratios of the active components, their concentration and the nature of the support on the physicochemical properties of the catalyst, looking for correlations between these properties and catalytic performance. In addition to the chemical composition, the analysis included the nature and morphology of the solid phases, the concentration of the active elements at the catalyst surface, with respect to the bulk, the surface acidity, the source of the electron spin resonance signal and the surface area and porosity of the solid.

Experimental

Analytical-grade reagents, deionised water and commercial aluminas were employed for the preparation of the catalyst. The procedure followed in the preparation and the fixed-bed reactor assembly employed for the activity test runs are described in detail in previous papers.[1,2] Briefly, Sb_2O_3 was refluxed in hot HNO_3. The Sb_2O_5 thus obtained was washed and a solution of V^{5+} and Mn^{2+} added, together with the support particles. Drying and calcination up to 923 K in air followed. In some cases the support was replaced by a mixture of montmorillonite and Cab-O-Sil.

Chemical analysis was carried out by standard spectrophotometric procedures[3,4] after dissolution of the sample by attack with $KHSO_4$. X-Ray diffraction (XRD) analysis (Debye method, Cu K_α radiation, Ni filtered) was carried out on a Philips PW 1700/00 diffractometer. The diffractograms were compared with those of pure supports and with literature data[5] in order to confirm or exclude the presence of known phases in crystalline form. Scanning electron microscopy–electron probe microanalysis

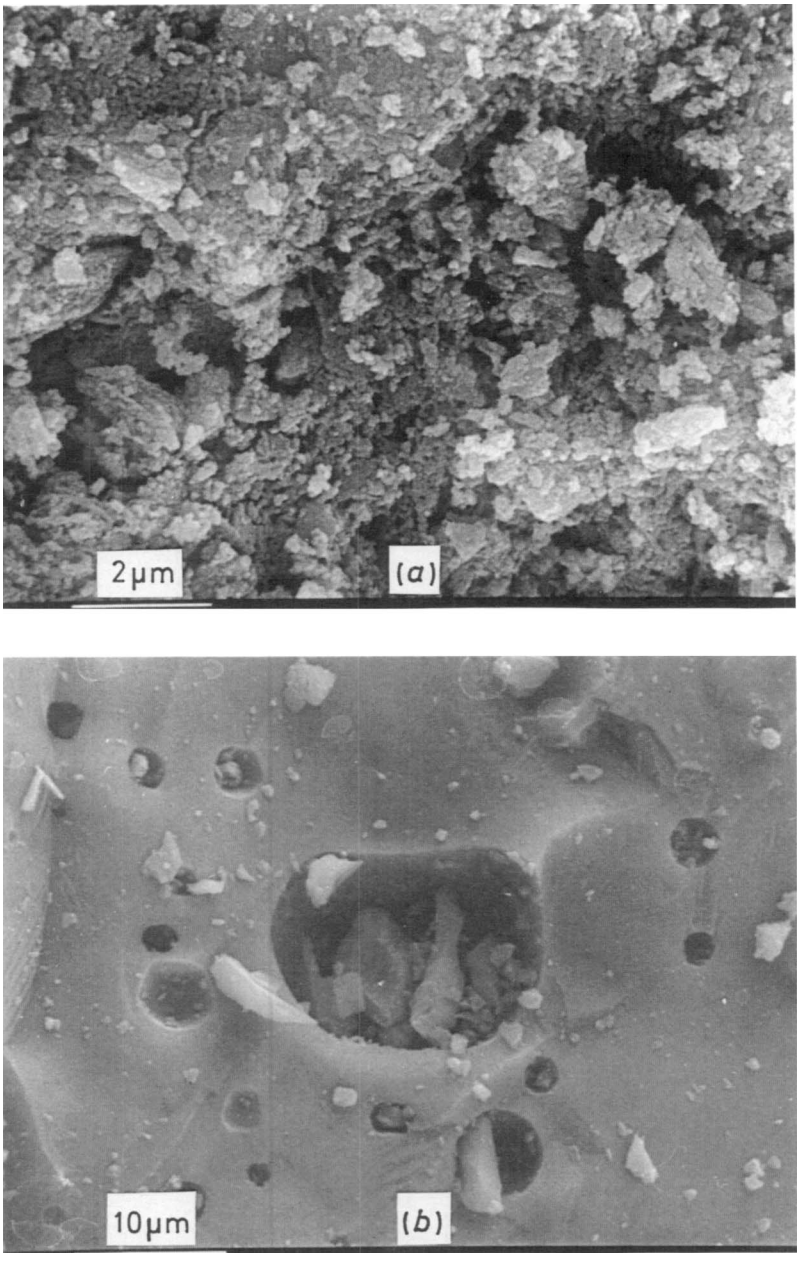

Plate 1. Typical SEM micrograph of: (*a*) catalyst A2, supported on AMC Carborundum alumina; (*b*) pure AMC alumina.

(SEM–EPMA) was made using a Cambridge Stereoscan 150-Link apparatus. The surface acidity was measured by titration with n-butylamine in an anhydrous solvent, after thorough outgassing *in vacuo* at 523 K. The B.E.T. surface area and porosity were determined by nitrogen sorption–desorption at 77 K. Electron spin resonance (e.s.r.) spectra were obtained by means of a Varian E-line Century series spectrometer.

Results and Discussion

Twelve different catalysts were prepared, analysed and tested. Their chemical compositions are reported in table 1. Their catalytic behaviour is expressed in terms of the conversion C (in mol %) of MP and the selectivity S (in mol % of MP converted) or yield Y (in mol % of MP fed), to CP. Each set of activity comparison runs was carried out under rigorously identical conditions, *i.e.* at 643 K and by feeding the same mixture of reactants ($MP:NH_3:air:H_2O = 1:2:75:10$ molar ratios).

Chemical analysis showed (table 1) that the compositions of the catalysts were always different from nominal. The differences are due to two main reasons: the incomplete recovery of some components, especially Mn and Sb, and a partial dissolution of the support (or binder) and of the freshly prepared Sb_2O_5 during the preparation procedure. In particular, the Sb/Mn and Sb/V atomic ratios that resulted were systematically lower, except for the unsupported, unbound B4 catalyst. The V/Mn ratio was systematically higher than nominal. Furthermore, the overall concentration of active oxides was higher than nominal for all catalysts, except A1 and C1. Nevertheless, fig. 1 shows that, when changing the nature of the support (A-series catalysts, table 1), the activity, referred to the unit mass of active oxides, seems practically inversely proportional to the amount of active components mounted on the support, while the yield is strongly dependent on the nature of the latter. For example, catalyst A1, whose support (T-60 alumina) seems also to be the most resistant (see data in table 1), is 2–4 times more selective than catalysts with other supports. A similar trend is observed by plotting the yield referred to unit surface area (fig. 1).

XRD analysis showed, in addition to the pattern due to the support itself, only the presence of α-Sb_2O_4 (a cervantite-like structure) and $SbVO_4$[5] in three of the four catalysts of the A-series (see *e.g.* fig. 2). For the fourth catalyst (A3, fig. 3) no diffraction lines corresponding to α-Sb_2O_4 or to other known phases containing Sb, such as Sb_2O_5, Sb_6O_{13}, Sb_2O_3 (senarmontite-like), α-Sb_2O_3 (valentinite-like) and particularly β-Sb_2O_4, could be found. Of course, this cannot exclude the presence of such phases in some micro- or submicro-crystalline form. As a consequence, it seem unreliable to correlate the catalytic activity to a particular crystalline phase. The only conclusion one can draw is that activity is connected with the presence of the Sb^{4+} species. As mentioned in ref. (1), such a species is usually considered in the literature[6] as a formal oxidation state, determined by the simultaneous presence of Sb^{3+} and Sb^{5+} ions, alternating in the crystal lattice of the oxide. It is thermodynamically unstable, but sufficiently resistant, with respect to the reduction to the stable Sb^{3+}, at least up to 750–800 K, under at least 10^{-4} Pa oxygen partial pressure. It is formed when Sb_2O_5 is heated at *ca.* 750 K, through the intermediate Sb_6O_{13}.

The analysis by SEM, at various enlargements, up to the limiting value (*ca.* 50000 ×) allowed by the instrument, showed only aggregates of microcrystals, covering the surface of the support more or less uniformly. The images were practically indistinguishable for any of the catalysts (see *e.g.* plate 1), thus providing no useful information as to the influence of any of the parameters examined on the morphology of the catalyst.

The surface composition was obtained by EPMA. The calculation requires the values of the so-called *ZAF* correction factors. Such factors take into account the effect connected with (*a*) the atomic number (Z), due to the stopping power of the radiation

Table 1. Characteristics of the catalysts employed

catalyst	support or binder	active oxide (wt %) nominal	active oxide (wt %) found	Sb/V/Mn wt ratios nominal	Sb/V/Mn wt ratios found	S_{BET} /m^2 g^{-1}	surface acidity/μeq g^{-1} a	b	c	V_p/cm^3 g^{-1}
A1	T-60 AlCoA	5	4.3	18.3/1.9/1	12.9/3.9/1	0.9	12	56	93	0.05
A2	AMC Carbor.	5	12.0	18.3/1.9/1	14.3/10.6/1	1.0	12	69	143	0.08
A3	SA5202 Norton	5	8.6	18.3/1.9/1	12.0/2.7/1	1.4	10	20	147	0.02
A4	Al3980 Harshaw	5	7.8	18.3/1.9/1	10.8/2.6/1	4.4	17	89	151	0.09
B1	AMC Carbor.	2	9.5	18.3/1.9/1	3.6/2.9/1	0.4	10	87	159	0.03
B2	AMC Carbor.	10	11.8	18.3/1.9/1	16.9/4.5/1	1.7	10	31	194	0.02
B3	AMC Carbor.	20	22.9	18.3/1.9/1	12.4/5.4/1	2.1	21	56	286	0.05
B4	none	100	100	18.3/1.9/1	21.6/2.5/1	5.2	45	53	172	0.12
C1	montmorillonite +Cab-O-Sil	62	57.3	4.9/1.9/1	5.3/2.3/1	6.9	12	53	372	0.03
C2	montmorillonite +Cab-O-Sil	62	66.7	8.9/1.9/1	4.4/2.9/1	10.5	31	99	318	0.11
C3	montmorillonite +Cab-O-Sil	62	62.3	13.3/1.9/1	10.9/3.1/1	8.7	34	42	219	0.10
C4	montmorillonite +Cab-O-Sil	62	72.9	18.3/1.9/1	8.1/2.4/1	7.2	24	44	475	0.07

[a] $pK_a \leqslant -1.5$. [b] $pK_a \leqslant 6.8$. [c] $pK_a \leqslant 1.5$.

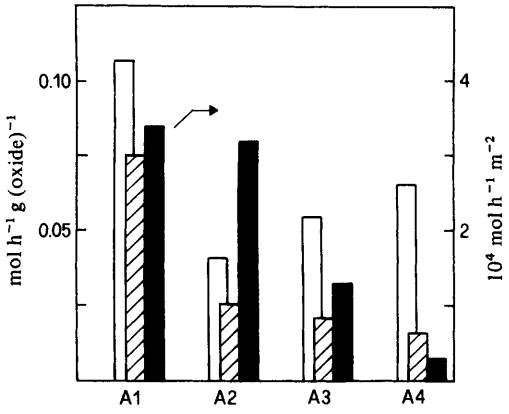

Fig. 1. Dependence of conversion (□), yield (▨) referred to unit weight of the active oxides and yield (■) referred to the unit B.E.T. surface area, on the nature of the support. A-Series catalysts (see table 1).

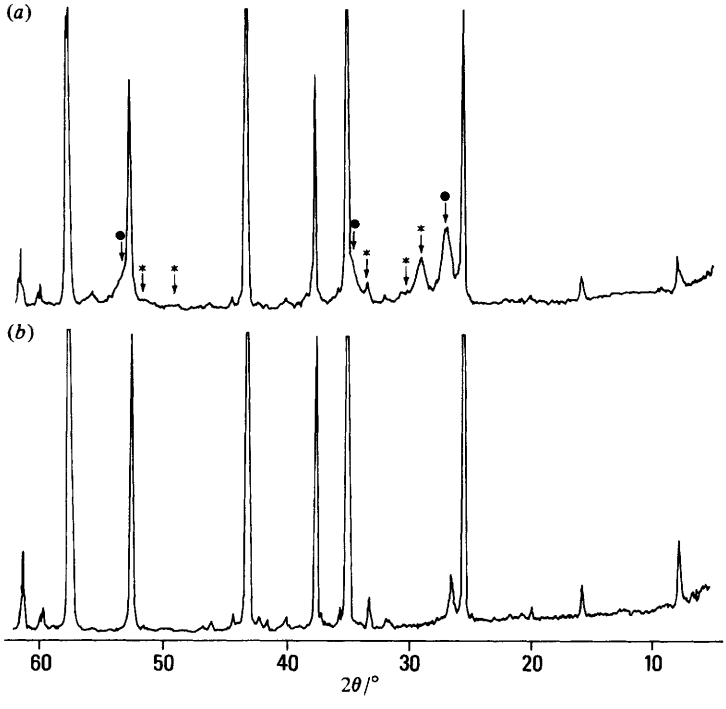

Fig. 2. Typical diffraction patterns of supported catalysts. (*a*) Catalyst A1, supported on T-60 alumina; (*b*) pure T-60 support. Diffraction lines corresponding to cervantite-like α-Sb_2O_4 (*) and to $SbVO_4$ (●) may be seen.

source and to the retrodiffusion of electrons, (*b*) the absorption (*A*) of the emerging radiation and (*c*) the secondary fluorescence (*F*). In the present case, only apparent correction factors for the three elements (Sb, V, Mn) were determined, by direct comparison of the spectrometric data of the various catalysts with those of catalyst B4. For the latter, owing to the absence of any support or binder, no segregation has been assumed due to these materials.

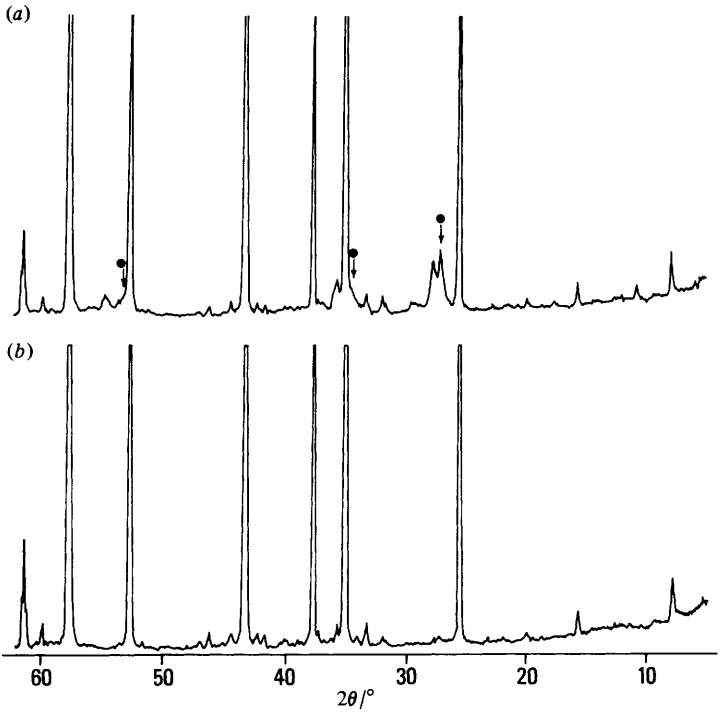

Fig. 3. Diffraction patterns of: (*a*) Catalyst A3, supported on SA5202 alumina; (*b*) pure SA5202 support. Only very weak diffraction lines (●), corresponding to $SbVO_4$, can be seen.

The surface concentration was calculated by averaging the results of 100 s counts, carried out, for each sample, on 20 different particles, enlarged at 1000 × magnification and by taking into account the *ZAF* correction factors determined as mentioned. The comparison of surface concentration with bulk composition, as obtained by chemical analysis, is shown in fig. 4. One may see that, except in one case (catalyst B2), Sb and Mn exhibit little segregation at any concentration [fig. 4(b)]. On the other hand, V seems to be more dilute at the surface, with respect to the bulk, in many of the supported catalysts [fig. 4(*a*) and (*c*)]. Of course, this effect may be in part only apparent, owing to the mentioned assumption of considering the unsupported catalyst chosen as standard to be virtually unsegregated. However, it seems undeniable, especially if one considers the V/Mn ratio [fig. 4(*c*)], from which it may be seen that the higher the concentration of V the more evident the phenomenon becomes.

The effect of the nature of the support on the surface area and porosity is shown in fig. 5 and 6. The selectivity, and hence the specific yield Y_s, referred to unit surface area, strongly increase with decreasing surface area (fig. 5). Furthermore, all the supported catalysts exhibit a bimodal distribution of porosity (fig. 6), but with different values of specific volume (from *ca.* 0.05 to *ca.* 0.09 $cm^9\ g^{-1}$) and surface area (from *ca.* 1 to *ca.* 4.4 $m^2\ g^{-1}$), with respect to the unsupported catalyst (B4), the latter showing values of 0.12 $cm^3\ g^{-1}$ and 5.2 $m^2\ g^{-1}$, respectively. An important point is the presence or absence of micropores ($10 < R_P/\text{Å} < 30$). When dealing with highly exothermic reactions, as in the present case, the presence of these pores may seriously reduce the selectivity to the desired partial oxidation or ammoxidation products. Indeed, by comparing the specific yield Y_s, given by the unsupported catalyst (4.6 mol $h^{-1}\ m^{-2}$) with those given by various supported ones (fig. 5) it may be seen that the lower the degree of microporosity (fig. 6), the higher is Y_s.

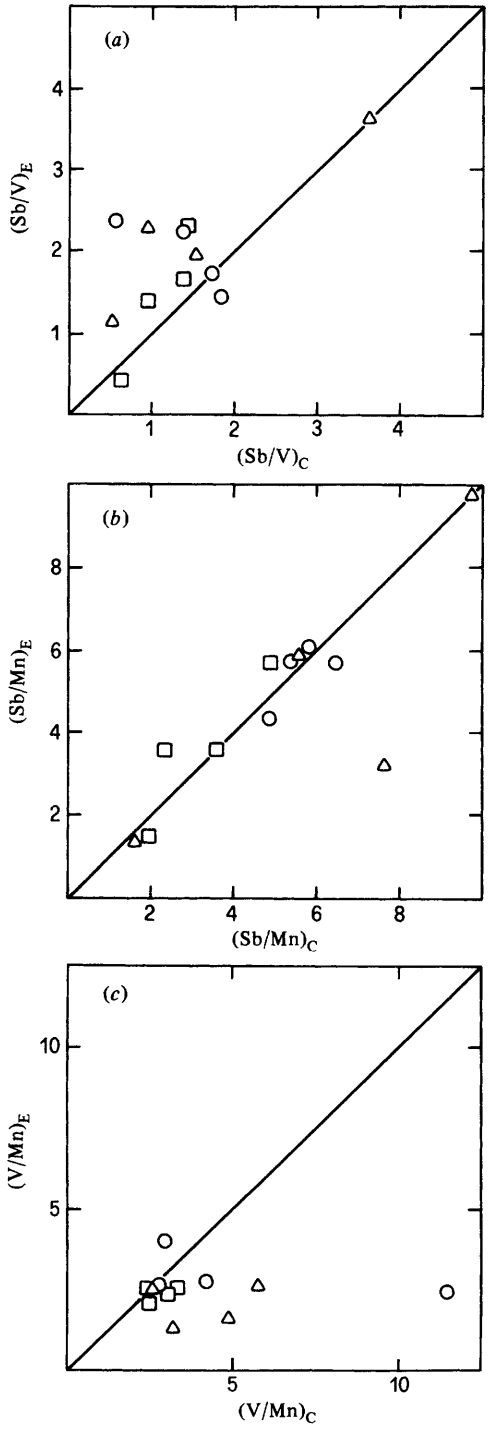

Fig. 4. Surface *vs.* bulk composition as determined by EPMA and chemical analysis (subscripts E and C, respectively): (*a*) Sb/V ratio, (*b*) Sb/Mn ratio and (*c*) V/Mn ratio, ○, △ and □ denote A-, B- and C-series catalysts, respectively.

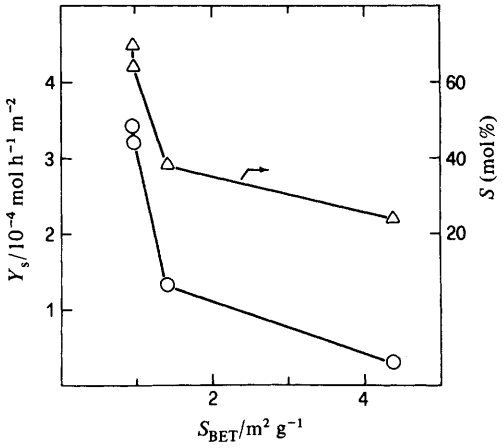

Fig. 5. Specific yield, Y_s, and selectivity *vs.* surface area (A-series catalysts, see table 1).

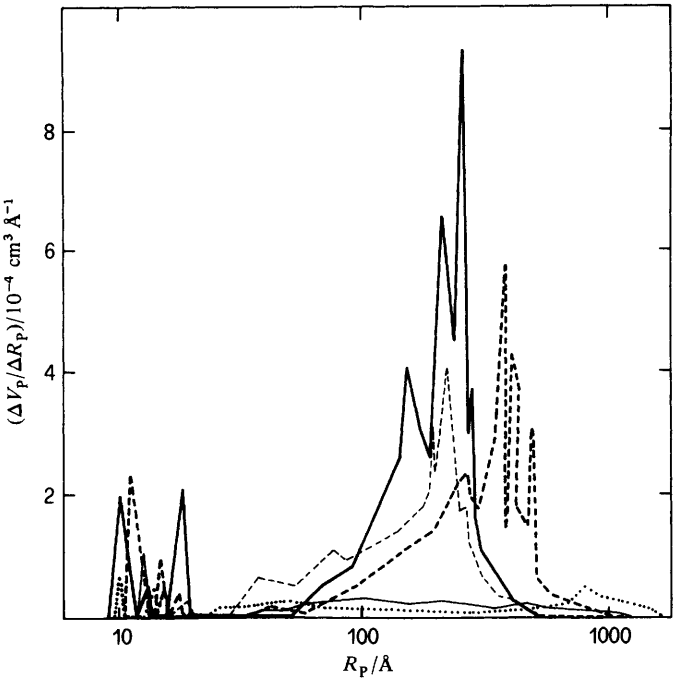

Fig. 6. Pore volume distribution of various supported (A-series) and unsupported (B4) catalysts. (···) A1, (——) A2, (——) A3, (– – –) A4, (– – –) B4.

The data for surface acidity titration are collected in table 1. However, for any of the catalysts, conversion and yield did not exhibit any particular dependence on the concentration of acid sites, irrespective of the acidity strength considered. Hence, acid sites do not seem to be directly involved in the present catalytic process.

The presence of unpaired electron species has been checked, as mentioned, by e.s.r. spectroscopy. All the samples were analysed between room temperature and 133 K. For all the supported catalysts, except A4, the spectra were almost identical at any

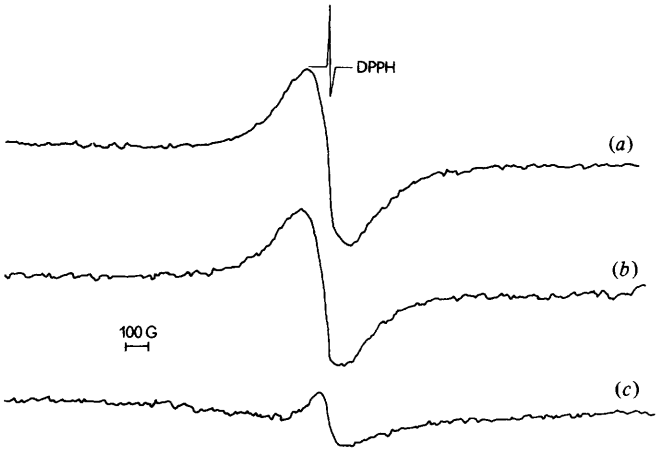

Fig. 7. Typical e.s.r. spectra of supported catalysts. Gain 16000. (*a*) Catalyst A1, 293 K; (*b*) Catalyst A1, 133 K; (*c*) pure V_2O_5 on the same support, 293 K.

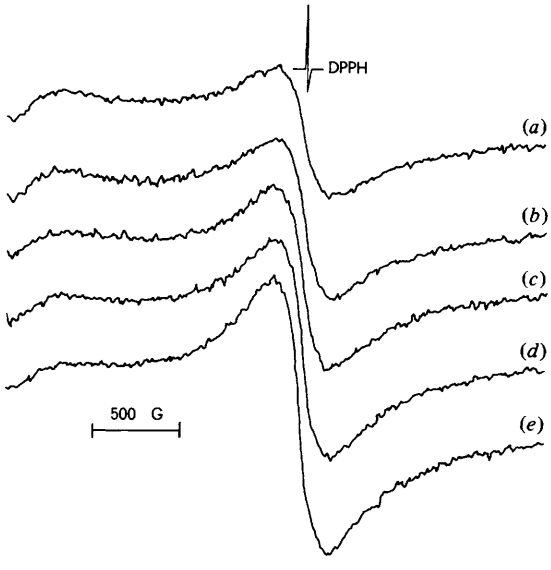

Fig. 8. E.s.r. spectra of catalyst A4. Gain 16000. Temperature: (*a*) 293, (*b*) 253, (*c*) 213, (*d*) 173 and (*e*) 133 K.

temperature [fig. 7(*a*) and (*b*)]. For the A4 catalyst, the series of spectra recorded by changing the temperature in 40 K steps, from 133 to 293 K, is shown in fig. 8.

The signal is always quite weak and is due to the presence of V^{4+} ions (H = 3000 G, $g = 1.97$). This has been confirmed by analysing a sample prepared by impregnating the same support with pure ammonium metavanadate, followed by calcination [spectrum (*c*) in fig. 7]. It is well known that solids containing unpaired electrons exhibit an e.s.r. signal, the intensity of which is inversely proportional to temperature for non-conductors and independent of temperature for electrical conductors. For semi-conductors, the e.s.r. signal grows in intensity as the Fermi level becomes more populated, passes through a maximum and then decreases when the number of electrons

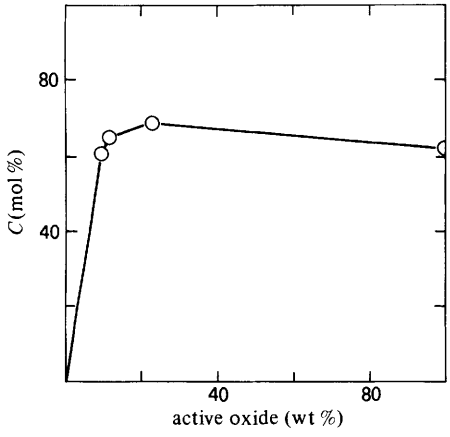

Fig. 9. Conversion as a function of active oxide charge on the same support (AMC alumina). B-series catalysts (see table 1).

present in the Fermi level increases further.[7,8] Note that the composition of both catalysts A3 and A4 (see table 1) is very close to the borderline separating the conducting and non-conducting behaviour of these oxide mixtures. As a consequence, a small change in the composition of these catalysts is sufficient to bring about a dramatic change in the electrical properties of the solid. In our system, the e.s.r. signal is due to V^{4+}, but the catalytic activity is closely connected with the presence of the Sb^{4+} (α-Sb_2O_4) species, the Sb^{3+} species being completely inactive.[1] The effect of V as a structural promoter may then be interpreted as producing a stabilisation of the formal Sb^{4+} state, by blocking or delaying its reduction to the thermodynamically stable, but useless Sb^{3+}. The e.s.r. spectra of our supported catalysts show that the active ones are essentially electrical conductors, the signal being independent of temperature. When the solid behaves as a non-conductor, *i.e.* when the e.s.r. signal is inversely proportional to temperature, the selectivity is strongly reduced, *e.g.* from > 70 mol % for catalyst A1, to < 25 % for catalyst A4. Hence, it may be concluded that the promoting action of V probably takes place by conferring electrical conductivity on the oxide mixture. As a consequence, the transfer of electrons from the bulk to the surface and *vice versa* is much easier, and the redox mechanism through which the catalytic action takes place is strongly enhanced.

The increase in concentration of active oxides on the support seems to have a much stronger effect on conversion than on selectivity, although it should be taken into account that, at least in part, the change in conversion is due to a variation in the Sb/V ratio (see *e.g.* catalyst B1 with respect to other members of the B-series). However, when plotting C *vs.* the charge of the active oxide (fig. 9), it may be seen that a concentration higher than 15–20 wt % does not improve the catalyst performance. By remembering[1] that the higher the concentration, the lower the mechanical strength of the catalyst, so that in the absence of any support the oxide mixture is very soft, it may be concluded that a concentration of *ca.* 10 wt % probably represents the best compromise between activity and acceptable mechanical strength.

Further interesting information is obtained by plotting the specific yield, Y_s, referred to unit surface area, given by the variously charged catalysts, *vs.* their B.E.T. surface area. An increase in Y_s is observed on increasing the latter parameter (fig. 10). These apparently surprising data may be explained by considering the trend of pore-volume distribution for such catalysts. The volume of mesopores (50–400 Å) regularly increases (from *ca.* 0.01 to 0.11 $cm^3\ g^{-1}$), on increasing the amount of oxide, but the ratio of

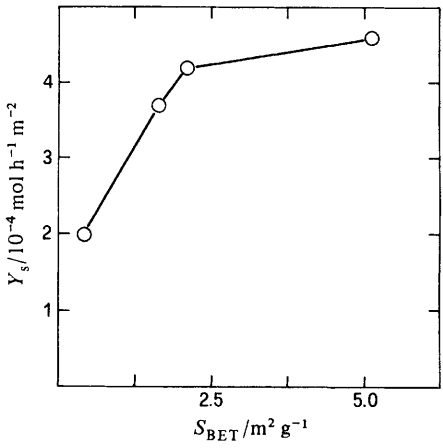

Fig. 10. Specific yield, Y_s, as a function of surface area. B-series catalysts (see table 1).

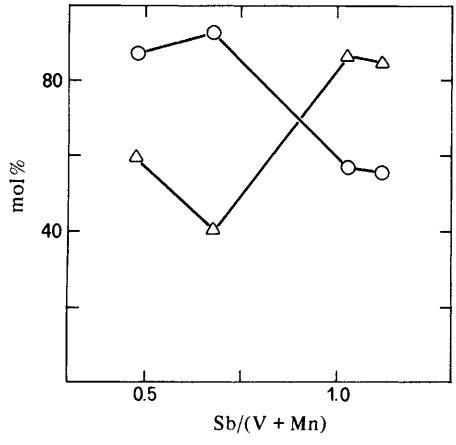

Fig. 11. Conversion (○) and selectivity (△) *vs.* the Sb/(V + Mn) atomic ratio. C-series catalysts (see table 1).

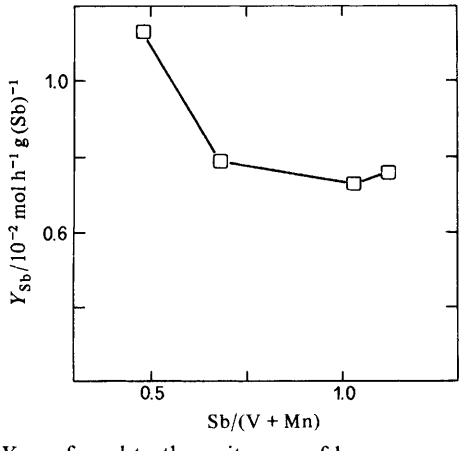

Fig. 12. Specific yield Y_{Sb}, referred to the unit mass of base-component (Sb), as a function of the Sb/(V + Mn) atomic ratio. C-series catalysts (see table 1).

micropore (10–30 Å) to mesopore volume becomes increasingly lower (0.050, 0.033 and 0.005, for catalysts B1, B2 and B3, respectively) with increasing amount of oxide, and micropores are totally absent in the unsupported (B4) catalyst (see fig. 6). Hence the negative influence on selectivity due to the presence of micropores becomes less important with increasing oxide charge.

Finally, the influence of the relative ratios among the active oxides on catalytic performance is shown in fig. 11. Conversion and selectivity show the usual opposite trend. Furthermore, if the specific yield, referred to the unit mass of Sb (Y_{Sb}), is plotted *vs.* the Sb/(V + Mn) atomic ratio, the effectiveness of the promoters can be readily observed (fig. 12). The higher the amount of promoters, the better the base compound (Sb) is exploited. However, it must be remembered[1] that, as in the absence of promoter, the catalyst life is considerably shortened when the previously mentioned atomic ratio is too low. A good compromise between performance and durability is thus attained when this ratio is not lower than unity.

Conclusions

The main results of the present work may be summarised as follows: (i) the support for this catalytic mixture should possess a very low surface area, such as T-60 AlCoA alumina; binders or high-surface-area materials should be avoided, in order to minimise side-reactions favoured by microporosity; (ii) a total amount of active oxides (Sb, V, Mn) of the order of 10 wt % of the finished catalyst probably corresponds to the best compromise between catalytic activity and mechanical strength of the solid; (iii) the true catalysts are probably antimony ions in the formal Sb^{4+} oxidation state, which is favoured by the presence of the promoters; (iv) the atomic ratio of the catalytic species Sb over the promoters should not be lower than unity, in order to exploit the active compound, whilst maintaining an acceptable catalyst life; (v) the catalyst should preferentially be an electrical conductor, a property which is conferred by the presence of V (and Mn).

Bracco Industria Chimica, Milano, is gratefully acknowledged for the research contract through which this work was carried out.

References

1 L. Forni, *Appl. Catal.*, 1986, **20**, 219.
2 L. Forni and F. Marzorati, *Ind. Eng. Chem., Proc. Des. Dev.*, 1985, **24**, 726.
3 *Treatise on Analytical Chemistry*, ed. I. M. Kolthoff and P. J. Elving (Wiley-Interscience, New York), part II, sect. A, vol. 8 (1963) and vol. 10 (1978).
4 A. Elkind, K. H. Gayer and D. F. Boltz, *Anal. Chem.*, 1953, **25**, 1744.
5 *Selected Powder Diffraction Data* (JCPDS, Swarthmore, PA, 1974), DBM/1/23 and PD 15–18 i. RB.
6 P. Pascal, *Nouveau Traité de Chimie Minérale* (Masson, Paris, 1958), vol. IX, p. 591.
7 J. M. Ziman, in *Principles of the Theory of Solids* (Cambridge University Press, Cambridge, 1965), p. 120.
8 C. Kittel, *Introduction to Solid State Physics* (Wiley, New York, 3rd edn, 1967), pp. 434 and 447.

Paper 7/1692; *Received* 21*st September*, 1987